EXPLAINABLE AI AND MULTI-OBJECTIVE OPTIMIZATION FOR ENERGY RETROFITS IN RESIDENTIAL NEIGHBORHOODS

JIAHONG YE [1], YANTING SHEN [2], CHENYU HUANG [3], JINYU WANG[4], RONG QU [5] and JIAWEI YAO [6]

[1,2,3,4,6]*College of Architecture and Urban Planning, Tongji University.*
[5]*China Construction Science and Industry Corporation LTD.*
[1]*yeesun_0v0@tongji.edu.cn*
[2]*sytsyt188@163.com*
[3]*cyhuang@tongji.edu.cn, 0000-0002-6360-638X*
[4]*johnwang1998@163.com*
[5]*qurong@cscec.com*
[6]*jiawei.yao@tongji.edu.cn, 0000-0001-7321-3128*

Abstract. Globally, the carbon emissions of building sector contribute to 40% of all. Therefore, low-carbon retrofits of buildings become pivotal to carbon neutrality. While existing retrofit research focus on individual building without considering whether different neighborhood morphologies would affect the effectiveness of retrofit strategies. Here we propose a framework for optimal retrofitting in diverse urban neighborhoods, balancing energy savings and cost. Based on actual residential neighborhood morphologies, massive parametric sample models have been established and batch simulated before and after the retrofitting for its energy performance. Then, we use XGBoost to establish a predictive model for energy savings, and iGeneS to perform multi-objective optimization. SHapley Additive exPlanations is utilized to reveal the nonlinear contribution of four retrofitting strategies to building retrofit benefits (BRB). Results demonstrate that in different floor area ratio (FAR), the contributions of installing rooftop photovoltaic panels to BRB vary. In neighborhoods with FAR of 1.5-2.8, the contribution of installing photovoltaic panels is not as significant as in other FAR ranges, and its contribution to BRB is not comparable to replacing energy-efficient lights. Moreover, The effectiveness of deep lighting fixture retrofitting may be suboptimal. The proposed framework will offer efficient energy-saving guidance for future residential neighborhood retrofits.

Keywords. Residential neighborhoods, Low-carbon retrofits, Urban morphology, Energy consumption, Explainable AI, Multi-objective optimization

ACCELERATED DESIGN, Proceedings of the 29th International Conference of the Association for Computer-Aided Architectural Design Research in Asia (CAADRIA) 2024, Volume 1, 485-494.

1. Introduction

Excessive energy consumption leads to an increase in greenhouse gas emissions, thereby exacerbating the climate crisis. Hence, a consensus has emerged among nations to adopt a low-carbon, and sustainable development model (Huang et al., 2022). Globally, the carbon emissions of building sector contribute to 40% of all carbon emissions (Lu et al., 2023). The urban development of China, the world's largest CO2 emitter, is gradually shifting towards urban renewal. Therefore, low-carbon retrofits become pivotal in attaining carbon neutrality. While current research on building retrofits tends to focus primarily on individual buildings, overlooking the potential impact of interactions among building clusters, and face challenges in reconciling the trade-off between energy savings and economic costs (Ma et al., 2023). So, a framework proposed in this study integrates explainable artificial intelligence (AI) and a multi-objective optimization algorithm to achieve the optimal retrofit solution, balancing energy savings and costs across diverse neighborhood morphologies. Furthermore, the study presents the marginal benefits of different strategies.

2. Related works

2.1. LOW-CARBON RETROFIT OF BUILDINGS.

Currently, existing research has explored low-carbon retrofit strategies for individual buildings (Gustavsson et al., 2022), such as enhancing the thermal insulation of the building envelope (Aruta, Giuseppe et al., 2023), installing rooftop photovoltaic panels, etc. However, the adaptability of various retrofit strategies varies across different neighborhoods. (Hong et al., 2020). For instance, high building density (BD) blocks can lead to shading, impacting photovoltaic efficiency. while, Low BD neighborhoods might increase the amount of heat entering through windows. In such cases, replacing glass with a lower Solar Heat Gain Coefficient (SHGC) is more effective for energy savings. Therefore, it is imperative to broaden the scale of the study of low-carbon retrofit strategies.

2.2. SURROGATE MODELS OF ENERGY CONSUMPTION

Obtaining building energy consumption data through simulation often consumes a significant amount of time. Therefore, many scholars are attempting to accelerate the acquisition of building model energy consumption data through alternative methods. (Liu et al., 2023). For instance, employing machine learning to develop urban energy prediction surrogate models that leverage city-specific feature metrics as input, enable the efficient prediction of building energy consumption (Huang et al., 2022). This approach significantly enhances the efficiency of energy consumption data acquisition.

2.3. EXPLAINABLE MACHINE LEARNING

Model explainability refers to the extent of human understanding of Machine Learning (ML) model predictions and decisions. Currently, the primary application of ML in the field of energy lies in energy consumption prediction. However, some researchers have combined machine learning with explainable analysis to guide design practices. For instance, by utilizing an ensemble algorithm that combines LightGBM with SHapley

Additive exPlanation (SHAP), various urban morphology indicators are explained in terms of their impact and contribution to urban energy consumption and carbon emissions (Zhang et al., 2023).

3. Methods

3.1. RESEARCH WORKFLOW

A framework proposed in this study integrates explainable AI and multi-objective optimization to attain the optimal retrofits solution in neighborhood morphologies. The optimization objectives encompass the maximum energy savings while minimum retrofits costs.

Firstly, this study prototypes real residential neighborhood morphology, constructing a batch of idealized sample models. Secondly, using Urban Weather Generator (UWG), Honeybee, and OpenStudio, the sample neighborhood models undergo two batches of performance simulations before and after retrofitting, and retrofitting costs are calculated. Subsequently, data on urban morphology parameters, retrofit strategy parameters, and energy savings are collected. XGBoost is employed to model the impact of urban morphology and four retrofit strategies on residential neighborhood energy savings, resulting in a predictive surrogate model for post-retrofit energy savings. Different forms of neighborhood retrofit strategies undergo multi-objective optimization to obtain post-retrofit Pareto solutions by multi-objective optimization plugin, iGeneS. Finally, XGBoost is utilized to model the impact of Pareto solutions' four retrofit strategies on residential neighborhood energy savings and retrofit costs. SHAP analysis is then applied to examine the nonlinear contributions of urban morphology and the four retrofit strategies to residential neighborhood energy savings and retrofitting cost when energy savings is the same. The research workflow is shown in the Fig 1.

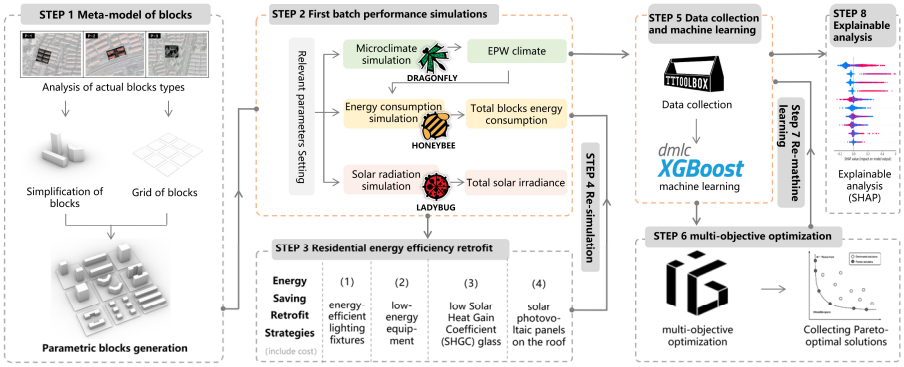

Figure 1. Workflow

3.2. RESEARCH OBJECT AND THE CONSTRUCTION OF A BATCH RESI-DENTIALMODELS.

Based on real urban morphology, an ideal residential neighborhood measuring 240m x 240m is planned within the Grasshopper. Subsequently, the land is divided into a 3 x 3 grid with 10m-wide roads. As shown in Figure 2, this study analyzes the residential building types in Shanghai and identifies nine typical morphologies. These include five categories of point-style residential clusters (P-1~P-5), two categories of slab-style residential clusters (S-1, S-2), and two categories of enclosure-style residential clusters (C-1, C-2). Next, these morphologies are simplified and randomly placed within the residential grid to generate a host of diverse sample models. The generated building heights are controlled between 3 and 25 floors, with a uniform floor height set at 3m.

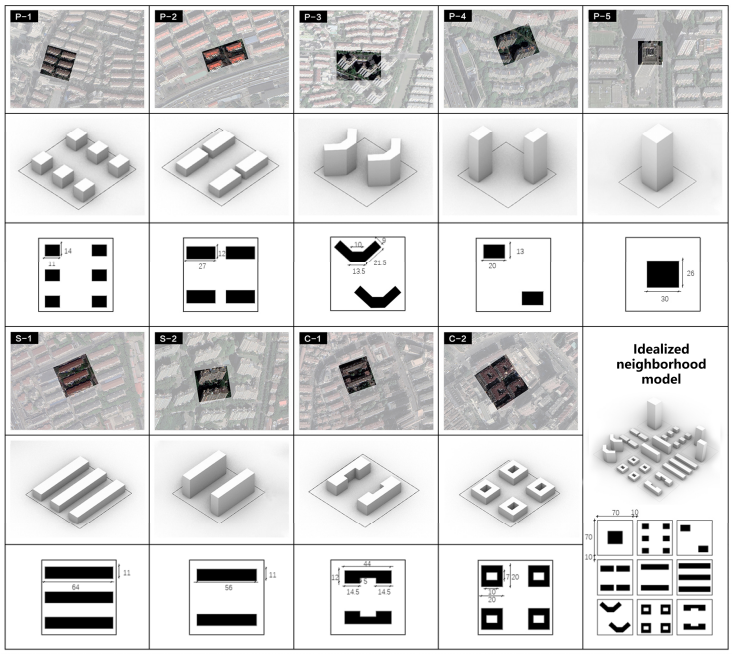

Figure 2. Samples of typical residential building types in Shanghai

3.3. INITIAL PERFORMANCE SIMULATION OF NEIGHBORHOODS

Using the Dragonfly and Honeybee, a large batch of sample models were transformed into UBEM. Based on previous research and the actual proportion of the actual distribution of residential functions (Liu et al., 2023), the idealized residential functional ratios are configured as follows: bedrooms accounting for 40%, living rooms for 20%, kitchens for 10%, bathrooms for 10%, and hallway spaces for 20%.

As shown in Table 1, this study, referencing relevant standards, sets the basic parameters of buildings before retrofitting. Additionally, considering the presence of the urban heat island effect, this research employed the UWG tool in energy simulations to conduct microclimate simulations of sampled neighborhoods for corresponding EPW climate files, which were then integrated with the parameterized UBEM and input into OpenStudio for simulations.

Table 1. Basic parameters of the buildings Before Retrofitting

Basic Information	Indicators	Parameters
Lighting	Lighting power density (w/㎡)	5.0
Equipment	Equipment power density (w/㎡)	3.8
People	Occupancy density (People/㎡)	0.04
Air Conditioning	Summer cooling temperature (℃)	26
	Winter heating temperature (℃)	18
Envelope	External wall heat transfer coefficient [w/(㎡ • k)]	0.8
	roof heat transfer coefficient [w/(㎡ • k)]	0.5
	partition wall heat transfer coefficient[w/(㎡ • k)]	1.5
	SHGC of glass	0.84
	glass heat transfer coefficient [w/(㎡ • k)]	2.7
Window-to-wall ratio	north-south window-to-wall ratio	0.4
	east-west window-to-wall ratio	0.1

3.4. LOW-CARBON RETROFIT AND RE-SIMULATION

This study applied four retrofitting strategies including utilizing energy-efficient lighting fixtures, low-energy equipment, low Solar Heat Gain Coefficient (SHGC) glass, and installing solar photovoltaic panels on the roof. Considering the actual situation, this study defined the post-retrofit parameter changes as follows: a reduction range for residential building lighting power density from 0 to 3.55 W/m² , a reduction range for equipment power density from 0 to 1.5 W/m² , a reduction range for glass SHGC from 0 to 0.7, and a power variation range for solar photovoltaic panels from 0.275 to 0.6 kW. Additionally, the study further categorized these retrofitting strategies into shallow, moderate, and deep retrofitting, with specific parameter range variation outlined in table 2.

Table 2. Range of retrofit parameter variations

	randomized retrofitting	Shallow retrofitting	Moderate retrofitting	Deep retrofitting
Reduction range of lighting power density (w/m²)	0-1.5	0-0.5	0.5-1	1-1.5
Reduction range of equipment power density(w/m²)	0.2-1.7	0.2-0.7	0.7-1.2	1.2-1.7
Reduction range of glass SHGC	0-0.7	0-0.233	0.233-0.466	0.46-0.7
Increase range of photovoltaic panel power (kw)	0.275-0.6	0.275-0.383	0.383-0.492	0.492-0.6

Based on market research, this study obtained retrofit costs (RC) calculation equations for different strategies through regression fitting (Equations 1-4). Following the completion of retrofitting, a second batch of performance simulations was conducted on the sampled models.

$$y_1 = -4.28x_1 + 27.76 \quad (1)$$

$$y_2 = -24.59x_2 + 89.61 \quad (2)$$

$$y_3 = -582.55x_3 + 504.02 \quad (3)$$

$$y_4 = 800x_4 + 331 \quad (4)$$

In the equations, $x_1$represents the post-retrofit lighting power density, $x_2$denotes the post-retrofit equipment power density, $x_3$represents the post-retrofit SHGC value of glass, and x_4 represents the post-retrofit power of the photovoltaic panels.

Additionally, y_1 signifies the cost of replacing energy-efficient lighting fixtures, y_2 represents the cost of replacing low-energy equipment, y_3 is the cost of replacing low-SHGC glass, and y_4 denotes the cost of adding photovoltaic panels.

3.5. CONSTRUCTING AN ENERGY PREDICTION SURROGATE MODEL

The TT toolbox plugin was employed to collect simulation datas, including morphological parameters such as Floor Area Ratio (FAR), Building Density (BD), as well as strategy-related variations like the differences in lighting and equipment power density. Additionally, data on retrofit costs of per square meter(RCM), changes in Energy Use Intensity before and after retrofitting(EUI_D), and Building Retrofitting Benefits (BRB) were collected. The calculation of BRB is as shown in equation 5.

$$BRB = \frac{\text{RCM}}{\text{EUI\_D}} \ (CNY/EUI) \tag{5}$$

Subsequently, XGBoost was applied to model the nonlinear relationships between neighborhood morphology, low-carbon retrofit strategy variables, and EUI_D. The models were evaluated using the coefficient of determination (R^2), resulting in surrogate models that map key design parameters to post-retrofit energy savings.

3.6. MULTI-OBJECTIVE OPTIMIZATION AND SHAP ANALYSIS

In this study, the iGeneS was employed in collaboration with surrogate models to achieve multi-objective optimization. IGeneS is a Grasshopper plugin capable of parallel computation, known for its fast execution speed and high convergence. The optimization parameters in this study included a population size of 100 and 100 generations for the number of iterations. The optimization objectives were set as maximizing EUI_D and minimizing RCM. The adjustable parameters are input parameters for the four retrofit strategies, including the decrease in lighting and equipment power density, glass SHGC reduction, and solar photovoltaic panel power increment.

Upon completion of multi-objective optimization, the Pareto solution sets data was output. Subsequently, XGBoost was applied to model the nonlinear relationships between neighborhood morphology, low-carbon retrofit strategies, and EUI_D and BRB. Following this, the SHAP was utilized to quantify the contributions of different low-carbon retrofit strategies to EUI_D and BRB.

4. Results

This study conducted low-carbon retrofitting and multi-objective optimization on 500 distinct urban morphologies, resulting in a total of 39,700 samples of Pareto solution data.

4.1. THE CORRELATION BETWEEN MORPHOLOGY AND EUI_D AND BRB

As shown in Figure 3, through Pearson correlation analysis, this study reveals the correlation between residential area morphology indicators and EUI_D and BRB. Specifically, BD, SD, OSR exhibit positive correlations with EUI_D and BRB, while FAR, AF exhibit negative correlations with EUI_D and BRB.

Figure 3. Correlation between morphological indicators and EUI_D and BRB

4.2. RETROFIT INTENSITY OF DIFFERENT NEIGBORHOODS

Due to the influence of morphology on EUI_D and BRB, and the presence of collinearity among some indicators, this study selects the commonly used FAR and BD to perform the following gradient division. Low FAR is defined as 0.7 to 1.5, medium FAR as 1.5 to 2.8, and high FAR as 2.8 to 4. The range for low BD is 0.15-0.22, medium BD is 0.22-0.3, and high BD is 0.3-0.4. Then, we further analyze the intensity of low-carbon retrofitting strategy selection under different morphologies.

4.2.1. Low-carbon Retrofitting Intensity under Different FAR

As illustrated by the distribution of Pareto solutions in Figure 4, this study observed minimal variations in the retrofitting intensity of glass, equipment, and lighting fixtures across different FAR for the four retrofitting strategies. Specifically, the retrofitting intensity for glass and equipment remained at a shallow level, while the lighting fixtures exhibited both shallow and moderate retrofitting intensities. The strategy involving the addition of solar panels showed variability in different FAR residential

areas; in low FAR neighborhood, a moderate retrofitting level is most suitable, while in medium to high FAR neighborhood, deep retrofitting could be considered.

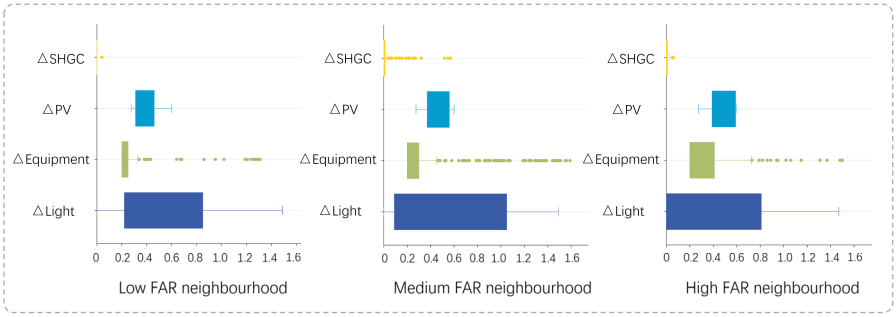

Figure 4. Distribution of retrofitting strategy intensity under different FAR

4.2.2. Low-carbon Retrofitting Intensity under Different BD

As shown in Figure 5, in different BD residential neighborhoods, there are variations in the adaptability of the four retrofitting strategies. Based on the analysis of the Pareto solution sets, this study found the retrofitting intensity for glass and equipment remained at a shallow level, while the retrofitting intensity for photovoltaic panels ranged from moderate to deep retrofitting. The retrofitting of lighting fixtures showed differences across different BD residential neighborhoods, with shallow and moderate retrofitting being suitable for medium to low BD neighborhoods, and medium to deep retrofitting being predominant in medium to high BD neighborhoods.

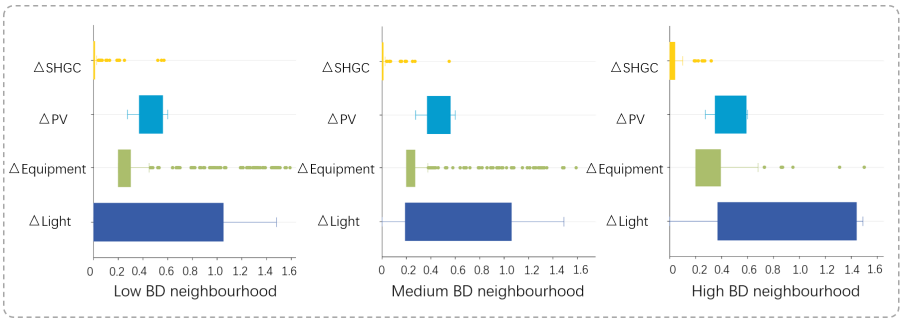

Figure 5. Distribution of retrofitting strategy intensity under different BD

4.3. DISPARITIES IN ENERGY-SAVING CONTRIBUTIONS OF DIFFERENT RETROFITTING STRATEGIES

4.3.1. Disparities in retrofitting strategy contributions in different FAR residential neighborhoods

Considering the optimal compromise between the two objectives in this study, various low-carbon retrofitting strategies demonstrate differences in their contributions to EUI_D across different FAR. As depicted in Figure 6, the strategy with the greatest EUI_D contribution in low FAR and high FAR residential neighborhoods is installing photovoltaic panels. However, in medium FAR residential neighborhoods, retrofitting lighting fixtures stands out as the most prominent contributor to EUI_D.

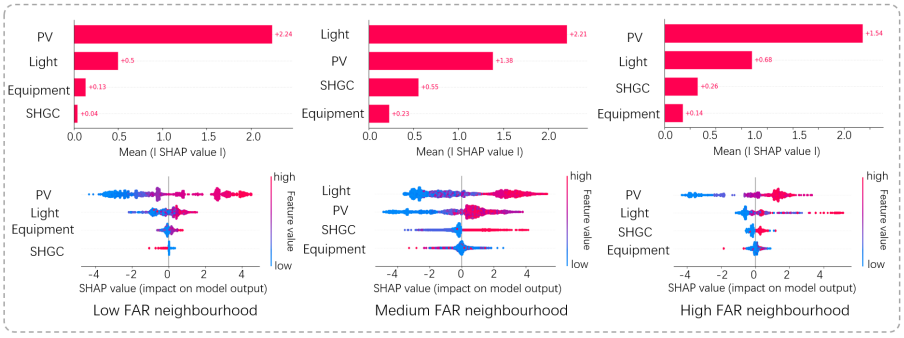

Figure 6. Retrofitting strategy contributions in different FAR

4.3.2. Disparities in retrofitting strategy contributions in different BD residential neighborhoods

Similarly, considering both retrofitting costs and energy savings, various retrofitting strategies exhibit differences in their contributions to energy savings across different BD. As illustrated in figure 7, in low BD residential neighborhoods, the strategy with the greatest energy-saving contribution is the replacement of energy-efficient lighting fixtures. However, in medium BD and high BD residential neighborhoods, the most prominent contribution installing photovoltaic panels.

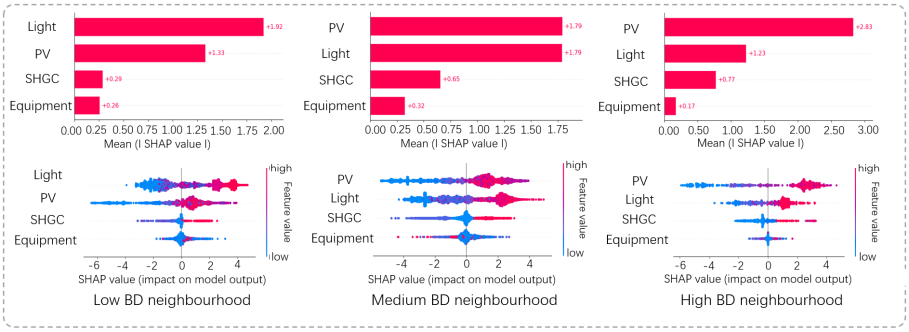

Figure 7. Retrofitting strategy contributions in different BD

5. Conclusion

This study aims to explore the adaptability and energy-saving contribution differences

of four strategies in residential neighborhoods. The results indicate that two retrofitting strategies, replacing low SHGC glass and upgrading to high-efficiency equipment, are prioritized for shallow retrofitting, while strategies involving the replacement of energy-efficient lighting fixtures and installing rooftop photovoltaic panels may be considered for moderate retrofitting. Additionally, installing the rooftop photovoltaic panels can be implemented for deep retrofitting in medium to high FAR residential neighborhoods. From an energy-saving contribution perspective, among the four energy-saving strategies in this study, prioritizing installing rooftop photovoltaic panels and the replacement of energy-efficient glass is most advantageous for enhancing the carbon reduction benefits.

The conclusions drawn in this study offer guidance for the retrofitting of neighborhoods, aimed at further enhancing the potential for low-carbon retrofitting. However, this study has certain limitations, such as drawing conclusions solely from simulations and without considering the causal effects between urban morphology, strategies, and energy savings. Therefore, future research will validate the findings using actual energy consumption data and incorporate causal inference into the research process to explore the comprehensive potential of various retrofitting strategies, promoting sustainable urban development.

Acknowledgements

This research was financially supported by the National Natural Science Foundation of China under Grant NO. 52278041 and the Fundamental Research Funds for the Central Universities.

References

Aruta, G., Ascione, F., Bianco, N., & Mauro, G. M., (2023). Sustainability and energy communities: Assessing the potential of building energy retrofit and renewables to lead the local energy transition. Energy, 282, 128377.

Gustavsson, L., & Piccardo, C., (2022). Cost optimized building energy retrofit measures and primary energy savings under different retrofitting materials, economic scenarios, and energy supply. Energies, 15(3), 1009.

Huang, C., Zhang, G., Yin, M., & Yao, J. (2022). Energy-driven intelligent generative urban design. CAADRIA, volume 1, 233-242.

Hong, T., Chen, Y., Luo, X., Luo, N., & Lee, S. H., (2020). Ten questions on urban building energy modeling. Building and Environment, 168, 106508.

Lu, Y., Chen, Q., Yu, M., Wu, Z., Huang, C., Fu, J., ... & Yao, J. (2023). Exploring spatial and environmental heterogeneity affecting energy consumption in commercial buildings using machine learning. Sustainable Cities and Society, 95, 104586.

Liu, K., Xu, X., Zhang, R., Kong, L., Wang, W., & Deng, W. (2023). Impact of urban form on building energy consumption and solar energy potential: A case study of residential blocks in Jianhu, China. Energy and Buildings, 280, 112727

Ma, D., Li, X., Lin, B., Zhu, Y., & Yue, S. (2023). A dynamic intelligent building retrofit decision-making model in response to climate change. Energy and Buildings, 284, 112832.

Zhang, Y., Teoh, B. K., Wu, M., Chen, J., & Zhang, L. (2023). Data-driven estimation of building energy consumption and GHG emissions using explainable artificial intelligence. Energy, 262, 125468